SIMPLE FORMATION CONTROL SCHEME TOLERANT TO COMMUNICATION FAILURES FOR SMALL UNMANNED AIR VEHICLES

Takuma Hino
***Dept. of Aeronautics and Astronautics, University of Tokyo**

Keywords: *Small UAV, Formation flight control, Virtual leader*

Abstract

In this paper, a simple but robust formation control scheme for small unmanned air vehicles is proposed. The proposed scheme is based on the virtual leader approach. Monte Carlo simulation showed that the proposed scheme allows formations with 95% of the possible communication networks to converge. Also, numerical simulations showed that proposed scheme allows formations to converge even if only 10% of the total communication succeeds. However, when aerodynamic interference between units were taken into account, the formation destabilised when trying to achieve maximum aerodynamic merit. Measures to stabilize the formation are currently under consideration. At the same time, flight tests are planned to demonstrate the proposed scheme and to obtain flight data to improve the mathematical model.

1 Introduction

Small unmanned air vehicles (UAVs), which are UAVs wingspans around 1 meter (Fig. 1 and Table 1) has been the one of the most researched groups of UAVs for the past decade. This is because small UAVs are easy and cheap to operate, as they do not necessarily require runways or large hangars. Therefore they are mainly used in missions which are either too dangerous or too expensive for manned aircraft too perform.

Despite these merits, not many small UAVs have entered public service. This is due to the small operation radii (around 50 km) and small payloads (around 500g) of small UAVs. One method to overcome these weaknesses is formation flight. Formation flight has the following four merits on operation of small UAVs. First, formation flight can reduce induced drag resulting in better fuel efficiency and larger operation radii. Aerodynamic analysis using vortex lattice method shows that formation of 5 UAVs can reduce up to 50% of induced drag, which leads to 40% longer cruise range (Fig. 2). Second, mission capability is not lost by a single aircraft failure, as the remaining units can carry on with the mission. Third, by distributing payload among units and cooperation, complex missions, which cannot be performed by a single aircraft, can be performed. Finally, for surveillance missions - which small UAVs are mostly used for, the mission execution time can be greatly reduced. For these reasons, a lot of research have already been done on formation flight and its control.

Fig. 1 Mitsubishi MARS07AF

Table 1 Specification of MARS07AF

Item	Value	Unit
Weight	2.00	kg
Wingspan	1.75	m
Wing area	0.392	m^2
Aspect ratio	7.7	
Cruise speed	15.0	m/s

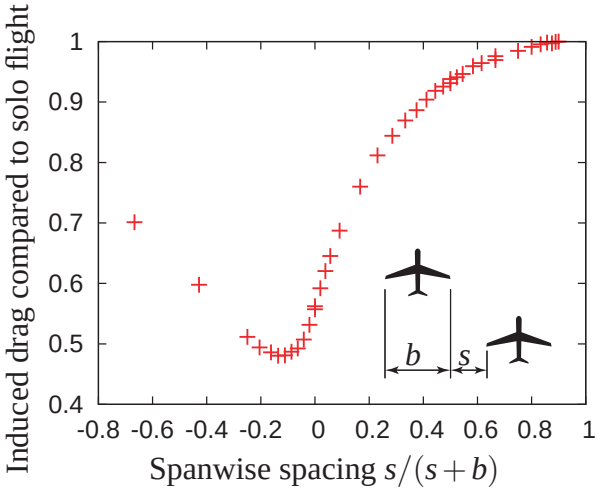

Fig. 2 Induced drag of 5 aircraft formation

Research on aerodynamic merits of formation flight have been done by Lissaman [6],Hummel [4] and Shevell [9]. Bloy [2] and Blake [1] focused on the interference between aircraft. They revealed that the interference destabilises the phugoid mode, and aircraft looses directional stability. In controlling formations, there have been two common approaches to it. – the leader follower approach and the virtual structure approach. The leader follower approach is simple but the leader being a point weakness within the formation. Therefore, this approach lacks robustness, which is essential for UAVs. The virtual structure approach taken by Lewis [5] and Ren [8], requires a large amount of calculation and in some cases, the calculation had to be done on a separate PC. As small computers used on small UAVs do not have high calculation power, this approach is also inappropriate to be used on small UAVs. Other researches include formation control with reduced communication (Xi [10]), formation by wake sensing (Pollini [7]) and analysis on information exchange within formation (Fax [3]).

In this paper, we will propose a simple formation control scheme based on the virtual leader (VL) approach, also taken by Xi [10], which can be performed on small UAVs feeble computer. We also combine it with point-to-multipoint communication to increase its robustness to communication failures and unit losses.

This paper is organized as follows. In section 2, the outline of the proposed scheme is described. Following that, the stability and convergence of the proposed scheme will be shown in section 2. Then in section 4, the robustness of the proposed scheme will be discussed. In section 5, numerical simulation is done to verify the performance of the proposed scheme. Finally, the paper is summarized in section 6 .

2 Control Scheme Outline

In the formation control scheme proposed in this paper, each unit has its own VL, which has its own dynamics. The proposed control scheme can be divided into two phases – the local control phase and the communication phase. The local control phase is the phase where each unit controls its position within the formation. In between the local control phase is the communication phase, where units exchange information to converge the formation into the desired shape (Fig. 3). The details of each phase are as follows.

1) Local Control Phase

Both formation members and their VLs are controlled by a state feedback controller so that they keep a specified relative position to each other. The VLs have an additional control input so that they track the desired course. For linear or locally linearized systems, this could be written as,

$$\frac{d}{dt}\begin{bmatrix} x^m_{l,i} \\ x^m_{f,i} \end{bmatrix} = \begin{bmatrix} A_l & 0 \\ 0 & A_f \end{bmatrix}\begin{bmatrix} x^m_{l,i} \\ x^m_{f,i} \end{bmatrix} - \begin{bmatrix} B_l & 0 \\ 0 & B_f \end{bmatrix}\begin{bmatrix} K_{ll} & K_{fl} \\ K_{lf} & K_{ff} \end{bmatrix}\left(\begin{bmatrix} x^m_{l,i} \\ x^m_{f,i} \end{bmatrix} - \begin{bmatrix} x_{l,i,t} \\ x_{f,i,t} \end{bmatrix}\right) \quad (1)$$

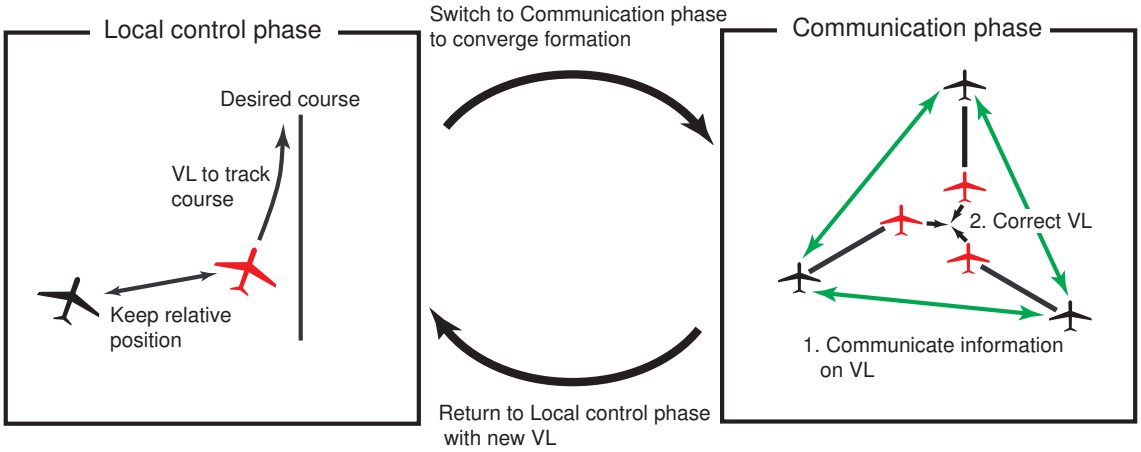

Fig. 3 Outline of proposed control scheme, Black = Formation members, Red = VL

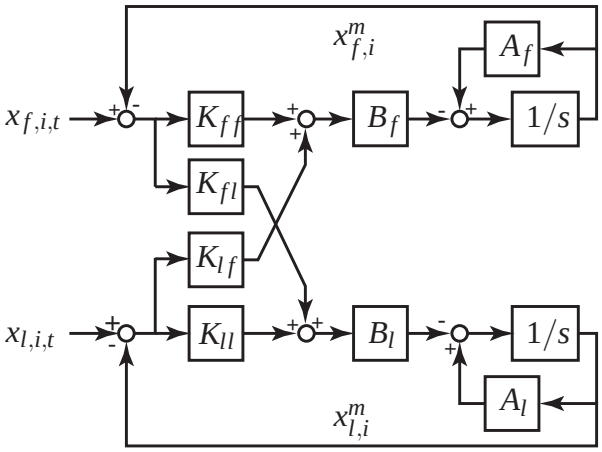

Fig. 4 Block diagram of state feedback controller for linear system

and drawn as Fig. 4. $x^m_{l,i}$ and $x^m_{f,i}$ are the state vector of ith unit and its VL after the mth communication phase. The two As are the system matrix and the two Bs are the control matrix, where suffix l is for formation members and suffix f is for the virtual leaders. The four K's are the feedback gains and $x_{l,i,targ}$ and $x_{f,i,targ}$ are the target values for $x^m_{l,i}$ and $x^m_{f,i}$ respectively.

The feedback gains are chosen so that the system (including VL) is stable. In another words,

$$Re(\lambda_k) \leq 0 \quad (k = 1, 2, \ldots) \tag{2}$$

where λ_k is the kth eigenvalue of the system.

2) Communication Phase

In each communication phase, all formation members will try to broadcast their VL's position using point-to-multipoint communication. When the ith unit receives information on jth unit's VL, it corrects its own VL as:

$$x^{m+0.5}_{f,i} = \frac{1}{2}\left(x^m_{f,i} + x^m_{f,j}\right) \tag{3}$$

$x^{m+0.5}_{f,l}$ represents the intermediate state between $x^m_{f,l}$ and $x^{m+1}_{f,l}$. If no information is received, then VL remains as it is. When all units have attempted to transmit information on their VL (end of communication round), the superscript incremented to $m+1$ and the next local control phase starts. Point-to-multipoint communication helps reduce the total number of transmissions required per communication phase.

By repeating these two steps, the VLs eventually converge into a single point, and formation members will be at their desired position to the VL. Hence, the formation will be in the desired shape, traveling along the desired path. Mathematical proof that the formation will converge will be given in the next section. As all units are equal and no point-weakness exists within the formation, the proposed scheme has a higher robustness compared to the leader follower approach. Also, the fact that only information on the VL is communicated, makes the scheme even more robust to communication failures.

3 Convergence and Robustness of the Proposed Scheme

In this section, mathematical proof on the convergence of the proposed scheme will be given, and numerical analysis on the robustness will be conducted.

3.1 Convergence of the Proposed Scheme

For the formation to converge into the desired shape, the VL must converge into a single point, and each member be at their specified position to the VL. As the feedback gains are chosen so that the system is stable, the latter condition will be satisfied after sufficient time. Therefore, only the former needs to be shown.

The degree of convergence of the VLs can be evaluated by the maximum distance between VL's state vectors after the mth communication round δ_m:

$$\delta^m(t) = \max_{i,j} |x^m_{f,i}(t) - x^m_{f,j}(t)| \tag{4}$$

where t is the time elapsed from the mth communication phase. Also, we will express VL's state vector as a linear combination of normalized eigenvectors v_k

$$x^m_{f,i}(t) = \sum_k \mu^m_{i,k} v_k \exp(\lambda_k t) \tag{5}$$

$$|v_k| = 1 \tag{6}$$

$\mu^m_{i,k}$ is the coefficient for the ith unit after the mth communication round. Subscript i is not required for the eigenvectors, as all units will be using the same feedback gain and therefore, the eigenvectors are identical throughout the formation.

For the VL to converge into a single point, δ^m has to converge to zero. Thus, we will prove the following theorem.

(Theorem)
δ^m is monotonically decreasing:

$$\delta^{m+1} \leq \delta^m \ (m = 0, 1, 2, \ldots.) \tag{7}$$

(Proof)
We will again, divide the proof into the two phases described in the previous section

1) Local Control Phase

From Eq.(2), the distance between VL's state vectors at time t after the mth communication phase will be,

$$\begin{aligned} |x^m_{f,i}(t) - x^m_{f,j}(t)| &= \left| \sum_k \left(\mu^m_{i,k} - \mu^m_{j,k} \right) v_k \exp \lambda_k t \right| \\ &\leq \sum_k \left| \mu^m_{i,k} - \mu^m_{j,k} \right| |v_k| \, |\exp \lambda_k t| \\ &\leq \sum_k \left| \mu^m_{i,k} - \mu^m_{j,k} \right| \\ &= |x^m_{f,i}(0) - x^m_{f,j}(0)| \end{aligned} \tag{8}$$

Thus

$$\begin{aligned} \delta^m(t) &= \max_{i,j} |x^m_{f,i}(t) - x^m_{f,j}(t)| \\ &\leq \max_{i,j} |x^m_{f,i}(0) - x^m_{f,j}(0)| \\ &= \delta^m(0) \end{aligned} \tag{9}$$

which shows that δ^m will not increase during the local control phase.

2) Communication Phase

Let S_k be the set of units that the kth unit succeeds to transmit information to. From Eq.(3), the distance between VLs will be

(a) when $j, k \in S_i$

$$\begin{aligned} |x^{m+0.5}_{f,j} - x^{m+0.5}_{f,k}| &= |\frac{1}{2} x^m_{f,j} - \frac{1}{2} x^m_{f,k}| \\ &= \frac{1}{2} |x^m_{f,j} - x^m_{f,k}| \end{aligned} \tag{10a}$$

(b) when $j \in S_i, k \notin S_i$

$$\begin{aligned} |x^{m+0.5}_{f,j} - x^{m+0.5}_{f,k}| &= |\frac{1}{2} x^m_{f,j} + \frac{1}{2} x^m_{f,i} - x^m_{f,k}| \\ &\leq \frac{1}{2} |x^m_{f,j} - x^m_{f,k}| + \frac{1}{2} |x^m_{f,i} - x^m_{f,k}| \end{aligned} \tag{10b}$$

(c) when $j \in S_i, k = i$

$$|x_{f,j}^{m+0.5} - x_{f,k}^{m+0.5}| = |\frac{1}{2}x_{f,j}^{m} - \frac{1}{2}x_{f,k}^{m}| = \frac{1}{2}|x_{f,j}^{m} - x_{f,k}^{m}| \quad (10c)$$

(d) when $j,k \notin S_i$

$$|x_{f,j}^{m+0.5} - x_{f,k}^{m+0.5}| = |x_{f,j}^{m} - x_{f,k}^{m}| \leq |x_{f,j}^{m} - x_{f,k}^{m}| \quad (10d)$$

Therefore,

$$\delta^{m+1} \leq \delta^{m} \quad (11)$$

From Eqs.(9) and (11), δ^m is proved to be monotonically decreasing.
(End of proof)

Alongside the fact that the formation members will be at their desired position to the VL after sufficient time, this proves that the proposed scheme will allow formations to converge.

4 Robustness of the Proposed Scheme

As noted in the previous section, the proposed scheme immune to unit failures, as there are no point-weaknesses within the formation. Also, the proof given in the previous section shows that the formation will converge if sufficient communication succeeds between units. These two properties will be demonstrated in the next section through numerical simulation. In this section, we will discuss the applicability of the proposed schemes to various communication networks, in another words, we will evaluate the number of communication networks which allows δ^m to converge to zero.

The evaluation is done numerically, by Monte Carlo simulation (MCS). Formation sizes between 3 and 15 units were evaluated, with 50,000 communication networks randomly generated in each case. The number of communication which allowed δ^m to converge to zero is listed in table 2. It can be seen in table 2 that the number of communication network which δ^m converged quickly increases with formation size, and for formation sizes over 13 units, no communication networks which δ^m did not converge were generated. This is because the more units there are, the more paths for information to be passed will be available. From this fact, it can be concluded that the proposed scheme can be applied to a extremely large number of formations and allow it to converge.

Table 2 Communication network evaluation results

No. of units	No. of cases which converged
3	39879/50000 (79.8%)
4	44181/50000 (88.4%)
5	47238/50000 (94.5%)
6	48977/50000 (98.0%)
7	49633/50000 (99.2%)
8	49879/50000 (100%)
9	49961/50000 (100%)
10	49990/50000 (100%)
11	49998/50000 (100%)
13	50000/50000 (100%)
15	50000/50000 (100%)

5 Numerical Simulation

Numerical simulations to verify the robustness of the proposed formation control scheme and to to see the effect of aerodynamic interference between units are carried out.

5.1 Numerical model

In the simulations, the formation members are assumed to be the small UAV shown in Fig. 1 and its specification given in Table 1 . The VL is assumed to be a simple 2D model, whose equation of motion is given as

$$\frac{\mathrm{d}}{\mathrm{d}t}\begin{bmatrix} x_e \\ y_e \\ V \\ \Theta \end{bmatrix} = \begin{bmatrix} V\sin\Theta \\ V\cos\Theta \\ \delta_t \\ \frac{V}{\pi B}\delta_r \end{bmatrix} \quad (12)$$

where B is the wheelbase, and δ_t and δ_r are the two control inputs. Other symbols are defined as in Fig. 5 and important simulation parameters are listed in Table 3.

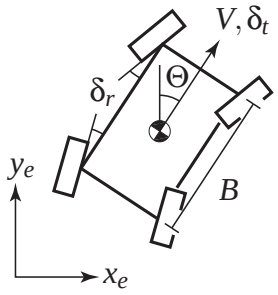

Fig. 5 VL Model

Table 3 Simulation parameters

Parameter	Unit	Value
Control update	Hz	50
Communication	Hz	2
B	m	0.4
Measurement noise (STD)		
Position	m	0.05
Speed	m/s	0.02
Attitude	rad	0.1
Disturbances (STD)		
Force	G	0.01
Moments	G·m	0.0001

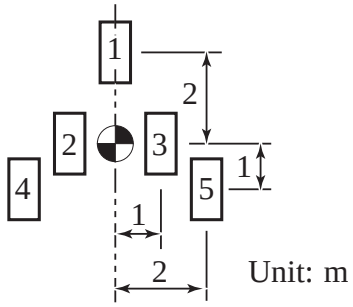

Fig. 6 Target formation

5.2 Simulation Scenarios

5.2.1 Robustness of proposed scheme

Five units are to form the formation shown in Fig. 6 (numbers inside rectangles are unit numbers) under the following cases.

Case 1 Form formation when 10% of total communications succeeds.

Case 2 Unit loss (unit 1) at $t = 30$s when 50% of total communications succeeds.

5.2.2 Effect of aerodynamic interference

Three units are to form formations shown in Figs. 9 and 10 with aerodynamic interference between units taken into account. For simplicity, only interference on forces and moments caused by displacement of units from their desired position were considered. The interference effects are calculated by vortex lattice method and expressed in a stability derivative form. In another words, the interference force (or moment) X on the ith unit is expressed as,

$$X_i = \sum \left(\frac{\partial X_{i,}}{\partial x_j} \Delta x_j + \frac{\partial X_{i,}}{\partial y_j} \Delta y_j + \frac{\partial X_{i,}}{\partial z_j} \Delta z_j \right) \quad (13)$$

where $\Delta x_j, \Delta y_j, \Delta z_j$ is the displacement of the jth unit from its desired position.

In all scenarios, the centre of gravity of the formation is to track the line $x_e = 0$.

5.3 Simulation Results

5.3.1 *Robust of the proposed scheme*

The simulation results are shown in Figs. 7 and 8 The position errors in the figures are the differences between actual position of units and their target position within the formation. In both cases, the formation settles into the desired shape, with position errors under 0.2[m]. This is a acceptable value, considering the measurement noise and disturbances. Figure 7 (*Case 1*) demonstrates the robustness of the control scheme to communication failures, where the formation is successfully formed even if only 10% of the communication succeeds. In Fig. 8, the formation is unaffected by the unit failure which occurs at $t = 30$[s]. These two results demonstrate the proposed scheme's robustness to unit failures.

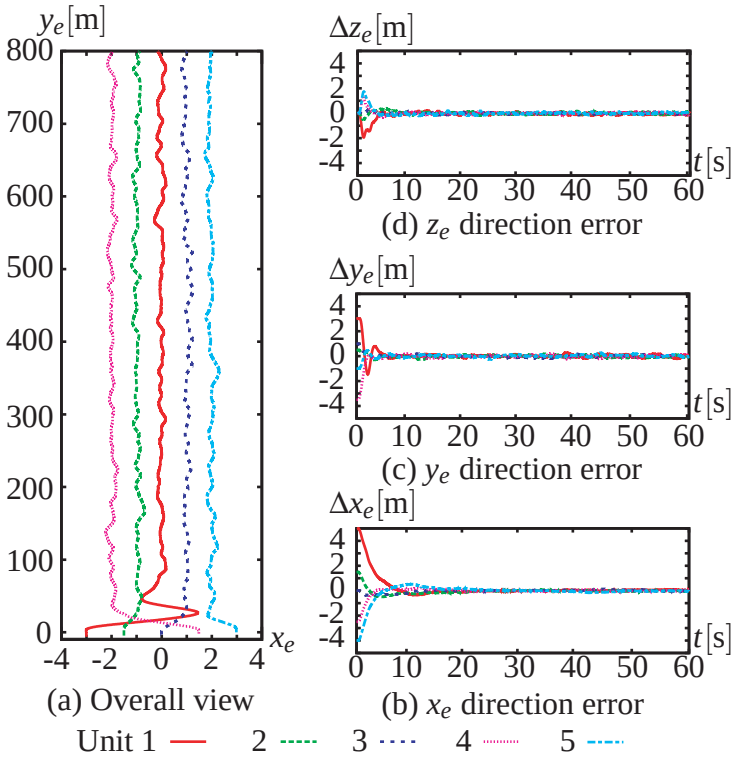

Fig. 7 *Case 1* 10% communication success

5.3.2 *Effect of aerodynamic interference*

The simulation results are shown in Figs. 11 and 12. When trying to obtain maximum drag reduction (Fig. 11), the interference between units destabilises the formation. This is because when the formation is packed extremely tight together in the spanwise direction, even the smallest spanwise displacements (Δys) lead to large drag changes which in turn leads to larger Δxs. On the other hand, when the drag reduction is compromised and the formation is spread out, the formation was still stable and showed the same performance as when no aerodynamic interference were taken into concern. However, for some feedback gains, the formation again became unstable. Thus, great care must be taken when choosing feedback gains, the interference between units must not be neglected.

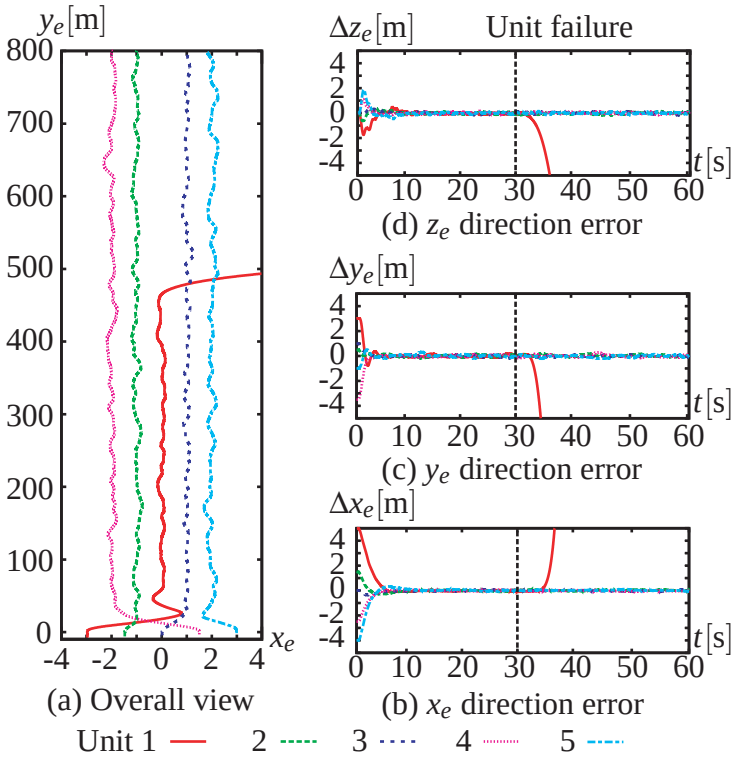

Fig. 8 *Case2* Unit 1 failure

6 Conclusion

In this paper, a simple formation control scheme using virtual leaders is proposed. In the proposed control scheme, formation members control their position to a common virtual leader and communicate information only on their virtual leader.

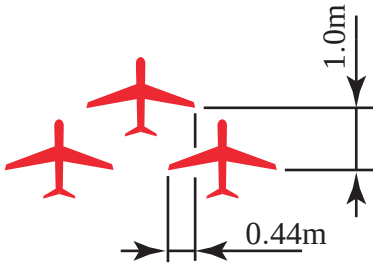

Fig. 9 Tight formation

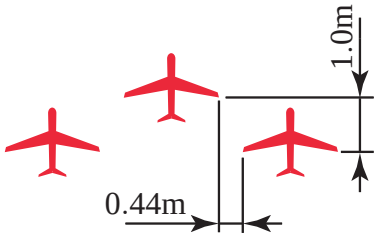

Fig. 10 Spread out formation

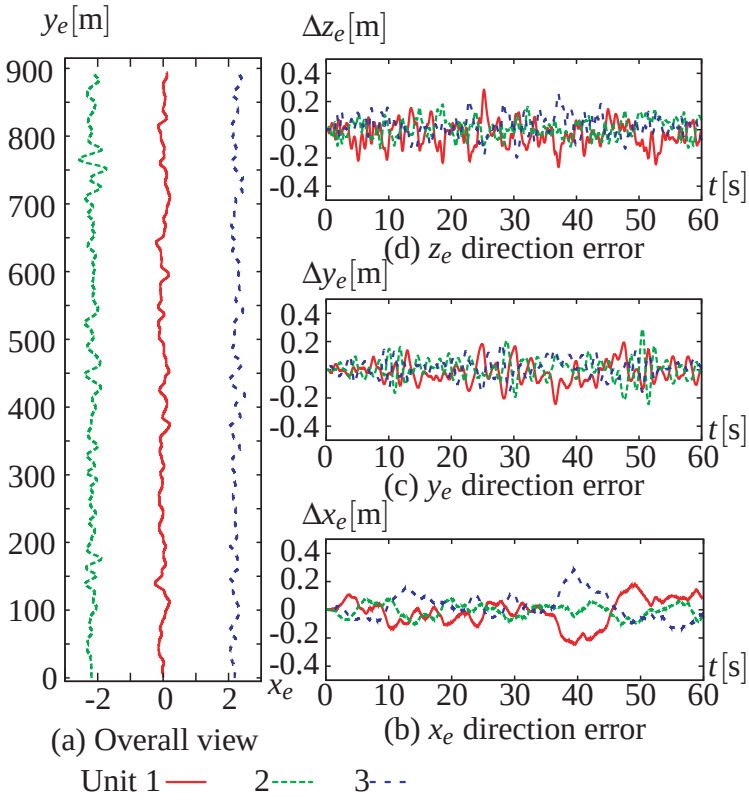

Fig. 12 Spread out formation with interference

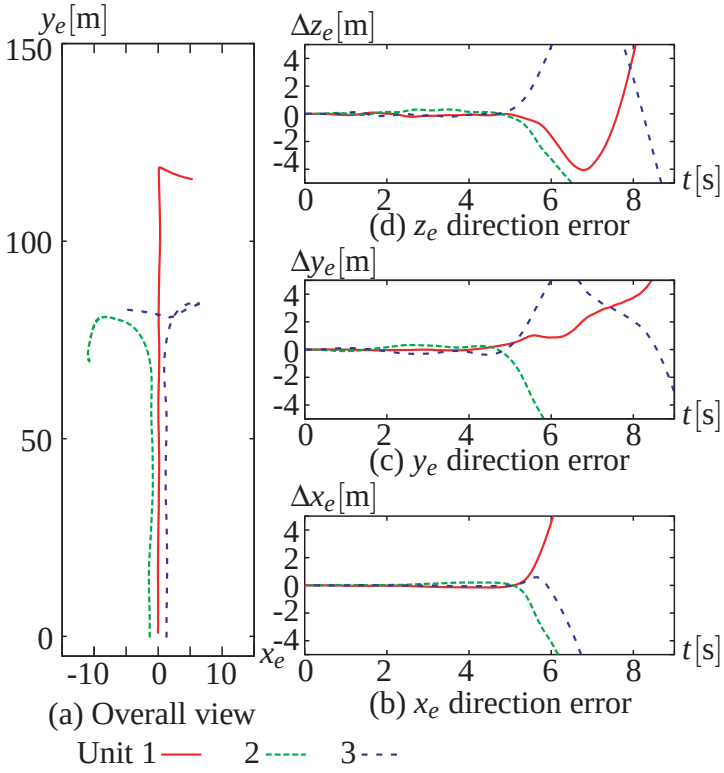

Fig. 11 Tight formation with interference

It was shown that the proposed scheme allows majority of formations to converge and that it can incorporate extremely high communication failures. Also, simulations showed that formations can be destabilised by interference between units and much care must be taken when choosing feedback gains. Furthermore, preparations for flight tests to actually demonstrate formation flight using the proposed scheme and to obtain information on the interference between units are currently underway. Autonomous flight by single UAV has just been achieved, and formation flight experiments are scheduled for late 2010.

References

[1] Blake W. B and Gingras D. R. Comparison of predicted and measured formation flight interference effects. *Journal of Aircraft*, Vol. 41, No 2, pp 201–207, 2004.

[2] Bloy A. W, West M. G, Lea K. A, and Jouma'a M. Lateral aerodynamic interference between

tanker and receiver in air-to-air refueling. *Journal of Aircraft*, Vol. 30, No 5, pp 705–710, 1993.

[3] Fax J. A and Murray R. M. Information flow and cooperative control of vehicle formation. *IEEE Transactions on Automatic Control*, Vol. 49, No 9, September 2004.

[4] Hummel D. Aerodynamic aspects of formation flight in birds. *Journal of Theoretical Biology*, Vol. 104, No 3, pp 321–47, 1983.

[5] Lewis M. A and Tan K.-H. High precision formation control of mobile robots using virtual structures. *Autonomous Robots*, Vol. 4, 1997.

[6] Lissaman P. B. S and Shollenberger C. A. Formation flight of birds. *Science*, , No 3934, pp 1003–5, May 1970.

[7] Pollini L, Giulietti F, and Innocenti M. Sensorless formation flight. *Proc AIAA Guidance, Navigation, and Control Conference and Exhibit*, 2001. AIAA 01-4356.

[8] Ren W and Beard R. W. Virtual structure based spacecraft formation control with formation feedback. *Proc AIAA Guidance, Navigation, and Control Conference and Exhibit*, 2002. AIAA 2002-4963.

[9] Shevell R. S. *Fundamentals of Flight*. 2nd edition, Prentice Hall, 1988.

[10] Xi X and Abed E. H. Formation control with virtual leaders and reduced communications. *Proc Proceedings of the 44th IEEE Conference on Decision and Control, and the European Control Conference*, pp 1854–1860, 2005.

Copyright Statement